C.P. No. 1254

C.P. No. 1254

MINISTRY OF DEFENCE (PROCUREMENT EXECUTIVE)

AERONAUTICAL RESEARCH COUNCIL

CURRENT PAPERS

An Omni-Directional Velocity Vector Probe suitable for use in Gas Turbine Combustors; Design Development and Preliminary Tests in a Model Combustor

By

J. J. Macfarlane

LONDON: HER MAJESTY'S STATIONERY OFFICE

1973

PRICE 70p NET

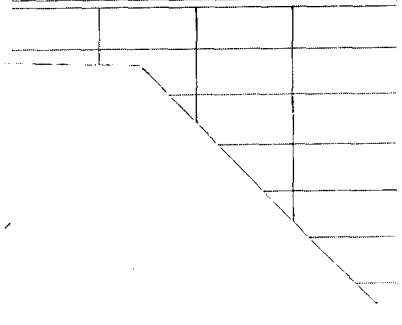

*C.P. No. 1254
October, 1971

An Omni-Directional Velocity Vector Probe suitable for use in Gas Turbine Combustors; Design Development and Preliminary Tests in a Model Combustor

- by -
J. J. Macfarlane

SUMMARY

A new technique is described which permits the construction of spherical multi-hole velocity vector probes in platinum/20% rhodium alloy. These probes are shown to be suitable for use at gas turbine primary flame temperatures while the head is sufficiently compact to permit the probe to be used in model combustor research. Starting with an established design of 5-hole probe, a programme of development is described which has led to a new design of 7-hole probe which can accept a vector from any direction in space. Tests were made in model primary zones to validate certain features of this design during its development and the results of these are described and discussed.

---

*Replaces A.R.C.33 887

CONTENTS

TABLES

ILLUSTRATIONS

ILLUSTRATIONS (cont'd)

1.0 Introduction

The need for the technique described in this Report arose in connection with the range of experimental model combustor primary zones[1,2] which have been developed at NGTE for studying problems arising in gas turbines at high pressures. These models operate in broadly the same way as full-scale gas turbine combustors, using the same basic techniques and covering the same range of operating conditions. In order to simplify the combustion process so that it can more readily be understood, unnecessary complexities in design are deliberately avoided. For example, the flame is stabilised by means of a closed toroidal vortex generated by an annular jet of primary air, admitted close to the periphery of the baseplate. These model primary zones can be operated over a wide range of air loadings and it was necessary to describe and quantify the way the flow regime varied with inlet conditions so that comparison could be made later with full-scale combustors.

The detailed flow behaviour of full-scale primary zones is not well established. Primary zone air quantity is deduced from areas and discharge coefficients of air injection holes and from measured or assumed values of local pressure drop. Information on the detailed flow pattern is derived from water models, is limited of course to isothermal conditions and is, in the main, purely qualitative although some attempts have been made to model fuel distribution by using chemical tracers[3].

For laboratory studies of Bunsen-type flames, extensive use has been made of small particles, injected into the air supply to the burner and observed photographically in the flame using lateral illumination and some form of rotary shutter to interrupt the light path at a suitable frequency. This gives regularly interrupted streaks on the photograph which can be used to measure particle velocity and direction. For gas velocity measurement, it is necessary, of course, to quantify the relation between particle and gas velocities. Tests of this method were made in the early stages of the present work. The principal limitation was found to be the reduction in the amount of light per unit area of photographic emulsion as particle velocity increased until, at a limiting velocity, no tracks were recorded. A considerable amount of interest has arisen recently in the possibilities of velocity measurement by observation of movement of particles seeded into the gas flow, observing the Döppler frequency produced when re-combining direct and particle deflected illumination in a Laser illuminated system[4]. This technique has considerable potential but, at the time of writing, is not sufficiently developed to provide a reliable routine tool.

There remains a family of methods, of varying complexity, based on pitot probe traversing. Here, the restricted access available through the sidewalls of a gas turbine combustor severely limits the type of probe design which can be used. Thus, techniques employing fairly simple, established types of pitot-static probes such as one of the NPL designs[5], which have been used successfully under conditions of good accessibility, are ruled out because of the need to provide a complicated traverse system to adjust the attitude of the probe in space to face the flow direction being measured. To simplify the traversing problem, various types of multiple pressure pitot probes of the claw, wedge or sphere type have been described for use in studies of three-dimensional cold gas flow.

Lee and Ash[6] describe a version of the widely used 5-hole spherical probe which appeared to be particularly attractive for use in the present problem. Their probe has a head diameter of only 5 mm and is calibrated so that, from a fixed attitude, it can be used to measure static pressure, flow velocity and direction over a range of angles of approach. The original probe was made in stainless steel and was used for studying cold flow in rotating cascades. The use of probes of this design under flame conditions was fostered by The International Flame Foundation at Ijmuiden and Pengelley[7] has described a water-cooled version with a sensing head some 19 mm diameter. The linear dimensions of typical gas turbine combustion systems are at least an order of magnitude smaller than those of the industrial furnace flames with which the Ijmuiden laboratories are concerned.

The present Report describes the construction of a probe of the same dimensions as the Lee and Ash probe but made from platinum/rhodium alloy which is suitable for use in stoichiometric hydrocarbon/air flames. The subsequent development of the aerodynamic design of the probe is described permitting the measurement of a velocity vector reaching the probe from any direction in space. The results obtained by applying these probes to model primary zone studies are discussed.

2.0 Method of construction used in making platinum/rhodium alloy probe heads

The reasoning adopted here was that the use of platinum/20% rhodium alloy, the melting point of which is 1875°C, would in itself give a structure which would withstand flame temperatures experienced over much of the gas turbine operating range. When this probe head is brazed to a water-cooled stainless steel arm, there is enough loss of heat by conduction to the cooling water to permit satisfactory operation at the maximum flame temperature in the kerosine/air range.

The technique of construction used is shown diagrammatically in Figure 1. The probe head is machined from 5 mm diameter platinum/20% rhodium alloy rod, the sphere being made in two pieces which are keyed together. Radial holes are drilled at appropriate points on the sphere to admit platinum/20% rhodium hypodermic tubing 0.76 mm o.d. and 0.40 mm i.d. which is threaded in a bundle through a central hole bored lengthwise in the shaft of the probe and individually, out through the five holes, set at the correct angles. Sufficient hypodermic tubing extends rearwards from the shaft to permit subsequent extension of these by stainless steel hypodermic tubes, the joints being nickel brazed.

The pieces of the platinum/rhodium alloy probe head (with the major dimensions left slightly over size) are thus assembled with the tips of the hypodermic tubes standing proud from the surface of the sphere. All the seams are then carefully welded together, using pure platinum welding wire (melting point 1769°C i.e. 106°C below the melting point of platinum/20% rhodium) using either a miniature argon arc welding torch or by electron beam welding. The assembled probe head is finish machined and, after nickel brazing the hypodermic extension tubes in position, the stainless steel tubular arm is joined to the head assembly by lower temperature brazing. The stainless steel tube passes through a cylindrical brass block (which carries a 360° scale to indicate angle of rotation of the probe on

its axis) to a cluster of 1/16 in. BSF vacuum unions. (W. Edwards & Co. Ltd.) These unions incorporate an 'O' ring seal and have proved to be reliably leak-proof while only requiring to be finger-tight. Cooling water connections to the jacket are via similar $\frac{1}{4}$ in. BSF unions. An assembled probe is shown in Figure 2.

3.0 Aerodynamic design and its effects on the operating range of the probe

Apart from mechanical reliability in a high temperature environment, there are two important requirements to be met in designing a velocity vector probe for use in combustion research. First, the direction of flow at a given point may be from any direction in space. In the simplest type of enclosed primary flow reversal, e.g. such as that produced by peripheral air admission, the flow describes an anchor-ring or torus-shape with the flow direction downstream near the confining walls and upstream near the axis in a radial, longitudinal plane, with little or no rotation about the axis. Various degrees of rotation may be imposed on this basic system by swirl vanes in the inlet air.

Secondly, access through the combustion wall is severely limited and complex movements to adjust the attitude of the probe relative to the combustor axis are out of the question. The fixed attitude operation offered by the probe described in Reference 6 is particularly attractive from this point of view.

3.1 The Lee and Ash probe

The layout of the probe head is shown diagrammatically in Figure 3. The probe axis is straight and the pressure points are arranged with one (hole 5) on the probe axis and the other four holes 90° apart and each at an angle of 40° from the probe axis. The operating principle is based on the relationship between the fraction of the free-stream dynamic head which will be indicated by a pressure tapping at the surface of the sphere (the pressure recovery factor K) and the angle θ between the axis of the pressure tapping and the flow direction. For a perfect sphere, these are related for a limited range of values of θ by the expression

$$K = 1 - \frac{9}{4} \sin^2 \theta \qquad \ldots.(1)$$

Values for K calculated from this expression, together with experimentally measured values obtained at one of the holes on the probe, are shown plotted against θ in Figure 4. The discontinuity in measured pressure recovery factor which occurs at about $\theta = 70°$ sets a limit to the range of values over which this probe can be used. Several factors can affect the usefulness of Equation (1) at values of θ less than 70°. It is easy to suffer small departures from spherical in manufacture at this small scale while the fact that the sphere is not isolated in space but is attached to the end of a probe at the point where the low pressure region would normally occur (i.e. the downstream face of the sphere) can be expected to reduce the

pressure gradient somewhat, as the data of Figure 4 suggests. It must also be remembered that the positions of the holes in the probe are related to any traverse mechanism or calibration jig via the shaft of the probe, and it is unreasonable to expect absolute precision in this relationship. All of this merely means that instead of calculating probe constants from first principles, it is better to employ empirical calibration of the probe as in the present work.

The flow direction is described by the two angles θ and δ where δ is a dihedral angle between a radial plane containing the flow direction and a meridian plane of the sphere (which is selected to be the plane which passes through holes 2, 5 and 4 in Figure 3). It can be shown[6] that these two angles are related to two expressions of the form

$$\frac{K_1 - K_3}{K_5 - K_3} = \frac{p_1 - p_3}{p_5 - p_3} \qquad \ldots.(2)$$

and

$$\frac{K_2 - K_4}{K_5 - K_3} = \frac{p_2 - p_4}{p_5 - p_3} \qquad \ldots.(3)$$

where the suffices 1 to 5 relate to hole numbers shown in Figure 3, p is pressure and K is pressure recovery factor.* These ratios have finite values when δ is between 0° and 180° but in the range 180° to 360°, the ratios become infinite when the vector makes equal angles with holes 5 and 3. For this reason, a second pair of ratios is used for $\delta = 180^\circ$ to 360°

$$\frac{K_1 - K_3}{K_5 - K_1} = \frac{p_1 - p_3}{p_5 - p_1} \qquad \ldots.(4)$$

$$\frac{K_2 - K_4}{K_5 - K_1} = \frac{p_2 - p_4}{p_5 - p_1} \qquad \ldots.(5)$$

The free stream velocity is related to the probe parameters by the expression

$$V = \sqrt{\frac{2g\ (p_5 - p_1)}{\rho\ (K_5 - K_1)}} \qquad \ldots.(6)$$

---

*In some texts, this is also referred to as the Static Pressure Coefficient (C_p)

or $$V = \sqrt{\frac{2g\ (p_5 - p_3)}{\rho\ (K_5 - K_3)}} \qquad \ldots.(7)$$

depending on the value of δ. where ρ = gas density

Static pressure is given by the expression

$$p_s = p_5 - K_5 \frac{\rho V^2}{2g} \qquad \ldots.(8)$$

g being the gravitational constant.

For calibration, the probe was placed with the centre of the sphere in the centre of the outlet plane of a 38 mm diameter nozzle (BS 1042) fed from a settling tank via a 1200 mm length of 75 mm i.d. pipe with a honeycomb flow straightener at the upstream end. The probe was held on a jig (Figure 5) which established the two angles θ and δ in relation to the nozzle axis. Uniformity of velocity at the nozzle exit plane was checked by means of a total head traverse. During calibration tests, velocities were calculated from air mass flow rate, measured by means of orifice plate meters with D and D/2 taps, made generally to the requirements of BS 1042 but using smaller pipe sizes than the specification minimum. These meters were calibrated against an equal areas total head traverse of a standard nozzle discharging to atmosphere.

The practical limit to θ in the resulting calibration chart (Figure 6) proved to be only 60° and it is therefore not possible to use this probe to traverse a flow reversal - it has to be possible to change the probe attitude. Added to this, a calibration of this kind is very time consuming to make and use.

3.2 Modified 5-hole probe for use at $\delta = 0$

A considerable simplification in calibration is obtained if the vector can always be arranged to lie somewhere in the plane of holes 1, 5 and 3. This can be done for vectors in one hemisphere if the pattern of pressure tappings is modified, as shown in Figure 7, in which hole 5 has been moved through an angle of 45° to the probe axis and the other four holes arranged again 40° from the axis of hole 5 and 90° apart. If now the probe is rotated in the air stream until the differential pressure between holes 2 and 4 is zero, the vector is located in the plane through holes 1, 5 and 3 and the calibration curve consists of a simple plot of Equations (2) and (4) above as a function of θ (in this case θ is still defined as the angle between the velocity vector and the probe axis).

It should be pointed out that there is a second value of δ, 180° away from the first one, at which the pressure differential between holes 2 and 4 is also zero. The angles between the vector and holes 1, 5 and 3 are larger in this case and the pressure recovery factors are recognisably more negative. Two similar probes have been made to this modified design and the measured calibration curves are sufficiently close to be represented by the single curve shown in Figure 8.

The results of extensive testing with this design in model combustors are discussed in Section 4.3 below. There are, however, some limitations on the way in which the probe can be used when traversing a flow reversal. The numerical value of pressure difference ratio derived from Equation (4) increases rapidly for vectors where θ exceeds 90° and tends towards $-\infty$ at $\theta = 100^{\circ}$ while that of Equation (2) tends to $+\infty$ at 10° beyond the probe axis (see Figure 8). The work discussed in Section 5.0 below was entirely concerned with axisymmetric systems and concentrated on measuring flow in the core of the reversal. Under these conditions, the range of vectors encountered could be kept within the compass of the limiting values of θ by traversing a selected radius as shown in Figure 9. Choice of the distance of the plane of traverse from the base plate was achieved by the device shown in Figure 9 but this was only made possible by the fairly simple geometry of the combustor. The probe would be much more widely useful if it could be inserted into the chamber axially from downstream, provided that its "angle of vision" could be substantially increased. It will be shown that this can be achieved by fitting two further pressure tappings and rotating the axis of the probe head a further 45°.

3.3 The 7-hole 'shepherds crook' probe

This development is best understood by referring to Figure 10. The shepherds crook arrangement is a well-tried one, permitting the sphere to be kept on the axis of the probe stem (so that it remains in one place when the stem is rotated) but permitting the operational axis of the probe head to be at 90° to the stem. What we have now done is to retain the old 5-hole pattern to centre on this operational axis and have added the two further pressure points, one 40° beyond the old hole 1 and the other 40° beyond the old hole 3. It is now more convenient to renumber the holes, as shown in Figure 10, so that the two 'yaw' holes for probe alignment by null reading become holes 6 and 7 while the holes in the vector plane are numbered 1 to 5. It will be appreciated that this row of five holes can be construed as comprising three separate systems of the kind used in the 5-hole probes and separate calibration curves can be drawn for holes 1, 2, 3; holes 2, 3, 4; and holes 3, 4, 5; as shown in Figure 11, although the middle curve does not really fulfil any essential function since there is adequate overlap between the outer two curves. It is still convenient to relate θ to the stem of the probe (rather than the axis of the sphere end which, in this case, is 90° different) because the stem is the only really suitable point on the probe to relate the orientation of the probe to its surroundings. Building the probe with 40° angles between measuring holes in this way means that there is 10° of traverse angle beyond each of the end holes and the pressure difference ratios tend to go into double figures in this region. There is not much magic in the 40° angle at this stage of development and by building the probe with 45° between holes 1/2, 2/3, 3/4 and 4/5 the limiting angle for pressure difference ratio to tend to infinity is deferred another 10° at each end of the scale, while still keeping a reasonable shape for the calibration curve at intermediate angles. The mechanics of calibration caused some difficulty at first, since once the probe is bent into a shepherds crook shape, it is impossible to carry the calibration beyond 105° using the jig shown in Figure 5. This difficulty was circumvented at first by carrying out the calibration before bending the probe. It was then realised that by replacing the 38 mm BS nozzle with the rather larger BS orifice plate, swinging the carrier bridge through 180° and fitting an extended pointer to the

scale of angles, the jig could be fitted to the suction side of a low pressure centrifugal blower casing so that the forbidden angles from 105° to 180° could be repeated on the bent probe (Figure 12).

We have thus arrived at a multi-hole probe design which has a fairly simple calibration and which can "see" in any direction and which is therefore not restricted to any particular location for introduction into a combustion system. To retain the ability to make a full rotation of the probe, it cannot be traversed closer to a confining wall than the outer radius of the shepherds crook. This restriction is overcome by a change in design to the form shown in Figure 13. This design can be fully rotated with the sphere only 3 mm from the combustor wall. To accommodate the internal connections to the extra two pressure points in this uncrooked design, the sphere diameter is increased from 5 to 6 mm. A calibration curve for this probe is shown in Figure 14.

3.4 Manufacturing precision and probe design repeatability

It has to be recognised that in making complex structures of small size by a welding technique, there is always a danger of mis-location of one or more pressure tappings due to thermal distortion. There was no sign of any trouble of this kind in the various 5-hole probes made and, as mentioned in Section 3.2, two probes made to the design of Figure 7 gave virtually identical calibration curves. In the 7-hole designs, holes 1 and 5 were much closer to the line of contact between the two parts of the sphere - in fact an experimental build was made in which this line of contact passed through holes 1 and 5 in the pre-weld condition. Under these circumstances, accurate placing of holes 1 and 5 is more difficult. Inspection by ordinary workshop means is not an easy matter but instructive deductions can be made from subsequent calibration data. The angular distribution of holes 1 to 5 was checked by replotting the pressures measured at individual holes, expressed as pressure recovery factor, against θ. The results are shown in Figure 15 which demonstrates that holes 1 and 5 are each some 10° closer to hole 3 than they should be. This particular variant of the manufacturing technique was therefore abandoned although it did offer some easement of the process of inserting the individual hypodermic tubes.

A useful standard of comparison was afforded in another case by a preliminary build which had been carried out in stainless steel, using low temperature brazing, a technique in which distortion should be absent. This is shown in Figure 16 side by side with a similar platinum/rhodium head in which holes 2 and 4 are badly out of alignment with holes 1, 3 and 5 due to overheating during manufacture. Comparison of the calibration curves for these heads (Figure 17) shows that this degree of distortion has not rendered the probe's performance unacceptable.

A further disadvantage of the shepherds crook design lies in the difficulty experienced in bending the shaft of the probe head (which is manufactured in the straight condition) so that the holes are correctly aligned relative to the stem of the probe. This can be observed by close comparison of the curves of Figure 11, which is a calibration made on a bent probe, with the full lines of Figure 17. The latter are from a calibration of a probe head before bending (i.e. while the hole position could be more accurately related to the axis of the stem). The curves of Figure 11 are

virtually identical to those of Figure 17 except that they are displaced to the right by some 7 or 8 degrees.

While the flow over the head of the shepherds crook 7-hole probe is undoubtedly cleaner, the final probe form is much more practical in its potential use in combustors. The amount of interference from the proximity of the probe stem to the pressure field in the region of hole 5 and to some extent hole 4 (see Figure 13) is not sufficient to interfere significantly with the probe's usefulness. Experiments in which the shape and distance from hole 5 of the profile of the probe stem was modified produced no significant change in calibration and the design does not appear to be sensitive to shape in this region.

4.0 Tests with model primary zones

The elaboration of these model primary zones is discussed in detail elsewhere[1,2] but a few words of explanation are required here. Although the work done covers a wide range of air throughput, some basic parameters have been kept constant throughout the series. The primary air is injected in each case from an annular nozzle 60 mm i.d., placed concentrically in a 75 mm diameter baseplate with a cylindrical combustor wall of the same i.d. Inlet air velocity at the nozzle exit is normally some 40 m/s although the effect of varying this in the range 20 to 120 m/s has been studied. In the work described in Reference 1 the combustor throughput was limited by the rather small fuel flows given by the special atomizer used to give monodisperse sprays. This limited air mass flow to rates in the range 0.5 to 3 g/s/bar. In more recent work an acoustic atomizer[8,9] is used and, since there is no longer a fuel flow limitation, combustor throughput has been increased (by about a factor of 10) and with it, air mass flow rate to give combustor residence times similar to those characteristic of current full-scale combustors. This range of air mass flow rates is accommodated simply by varying the width of the annular orifice to keep injection velocity constant. The general arrangement of the two baseplates is shown in Figure 18.

4.1 Pressure measurement techniques

For tests with model combustion chambers, the injection velocity of generally not greater than 120 m/s will represent the maximum free stream dynamic head for which pressure measurements must cater. Using the expression $h = \frac{\rho V^2}{2g} \times 10^4$ we can determine the range of values of h in millibars corresponding to a range of velocities (V) in m/s for both cold flow ($\rho = 1.16$ kg/m^3) and for stoichiometric combustion products at maximum flame temperature ($\rho = 0.16$ kg/m^3) the standard value for g being 9.806 m/s^2. This gives the following values of h

Velocity	Free stream dynamic head h (h = cm H_2O = millibars)	
m/s	Cold Flow	Hot Flow
0.3	0.0005	0.00007
1.0	0.0059	0.00081
3.0	0.053	0.0073
10.0	0.59	0.082
30.0	5.32	0.73
100.0	59	8.2
120.0	85	11.8

The lower limit of measurement will depend mainly on the level of noise experienced due to turbulence.

For much of the early exploratory work on this project, pressures were measured relative to atmospheric pressure using U tube manometers made in precision bore glass tubing, one for each pressure tapping on the probe. The manometer liquid used was absolute ethyl alcohol (specific gravity = 0.792) and measurements were made by means of a precise measuring microscope which was graduated every two micrometers. A 25 per cent error in measuring h at the 0.01 millibar level (corresponding to a 5 per cent error in a hot flow velocity of 3 m/s, which was adequate at this level) gives a limiting required sensitivity of pressure measurement of 0.0025 millibars, or 25 micrometers of water head. This is comfortably within the capability of the measuring microscope.

Measurements of this kind are inevitably slow, and presume a long-term stability of signal which, although available under calibration nozzle conditions, cannot be expected during routine measurements in a combustion chamber. A commercially available sensitive micromanometer, suitable for this kind of measurement, is described by Pengelley[10]. This is a diaphragm operated differential transformer type pressure transducer, which is fed from a 1000 Hertz, 22V, a.c. generator and gives a d.c. output signal of up to 1V for FSD after rectification.

The most sensitive model has a nominal range of 0 to 4 (or +2 to -2) millibars and the required sensitivity of ±0.0025 millibars represents 0.06 per cent FSD on this instrument. This compares with the maker's claim of ±0.02 per cent FSD maximum sensitivity and an inherent noise level, measured under quiet room conditions, of 0.04 per cent FSD.

A group of five of these +2 to -2 millibar range transducers was used in conjunction with a 5-hole probe of the type shown in Figure 7 for the experiments described in Section 4.2 below. Temperature difference effects were minimised by enclosing the transducers in a single aluminium block and the apparatus was switched on 2 hours before the start of a test to permit a steady operating condition to be reached. The transducers were interconnected with the five pressure tappings on the probe in such a way that the following information was read directly in this order

Transducer 1 Differential pressure between holes 2 and 4, for use in setting the probe to zero yaw angle

Transducer 2 Pressure at hole 5 (versus atmospheric)

Transducer 3 Differential pressure hole 1 - hole 3

Transducer 4 Differential pressure hole 5 - hole 3

Transducer 5 Differential pressure hole 5 - hole 1

Transducer sensitivity was checked against an absolute alcohol U tube manometer read with the measuring microscope.

4.2 Description of the model combustor

The layout of the test equipment is shown in Figure 9. The upper portion, consisting of a water-cooled outer jacket and thick-walled Nimonic 75 liner, carrying a mechanism for traversing the probe radially through a single, close fitting hole in the liner, is mounted on a brass plate 215 mm o.d. and having a 25 mm rim threaded on its outer surface. The lower part of the rig, which carries a similar flange threaded in the opposite hand, consists of the base plate of the combustor which is really the top surface of a 75 mm diameter plug, 60 mm long, which locates in a similar sized hole in the base of the upper part of the rig, by means of an 'O' ring seal. Three alternative widths of annular jet are provided; 0.20, 0.48 and 0.69 mm respectively. The upstream part of the annulus is 2.5 mm wide reducing to the narrower width for the last 10 mm length before eflux.

Propane gas can be fed axially into the central block of the plug and is distributed radially by means of an aluminium plate which has a large number of radial grooves engraved on its surface. This discharges into the air annulus at the point where the annulus width is reduced from 2.5 mm to the discharge nozzle size. The propane flow rate is monitored by an orifice meter, similar to the one used for airflow measurement. The metered fuel/air ratio was checked by comparing the calculated flame temperature derived from it, with values measured by means of an electrically compensated 20% rhodium/platinum/40% rhodium/platinum thermocouple[11]. The measured temperatures were consistently slightly higher than the calculated values, the mean difference from five readings covering the fuel/air ratio range 0.034 to 0.050 being $+35^{\circ}C$, $\pm 25^{\circ}C$. This is quite acceptable agreement for a measurement of this kind.

4.3 Test results

For each test condition, a set of probe pressures was measured every 2.5 mm along a radius of the combustor (see Section 3.2 above). Using the formulae given in Section 3.1, values of the two angles θ and δ and the velocity and static pressure were calculated at each point. Inspection showed the radial limit of the reversal core, characterised by a quite sharp change in flow direction. For each point, a resultant axial flow velocity was deduced and from these values, an area weighted mean velocity for the flow reversal core. Flame temperature was calculated from the measured mixture strength.

This, together with the observed static pressure, gave flame gas density and hence reversal mass flow rate. A set of readings of this kind

was taken for a range of inlet mass flow rates, both in cold flow and over a range of mixture strengths and these are shown in Table I. A similar set of data (in cold flow only) was measured using the baseplate shown in Figure 9b and these are shown in Table II.

The mass rate of flow in the core of the recirculation set up by a confined annular jet can be equated to the mass rate of entrainment into the primary jet. It is legitimate to consider an unconfined annular jet, in which the thickness of the annulus is small compared with its radius, as geometrically similar to a plane two-dimensional jet as Cox has pointed out in Reference 12. However, it is more reasonable to treat the present jet as entraining air on its inside surface only in which case its behaviour approximates closely to that of a simple round jet (turned inside out, so to speak) and the treatment devised by Ricou and Spalding[13] can be used. From a dimensional analysis of the system, these authors deduced that the mass flow rate (q) of the jet increases with axial distance (x) according to the expression.

$$\frac{q_1}{q_o} \propto \frac{x}{r_o}\left(\frac{\rho_1}{\rho_o}\right)^{\frac{1}{2}} \qquad \ldots.(9)$$

Since $$\frac{\rho_1}{\rho_o} \propto \frac{T_o}{T_1}$$

Equation (9) can be written $$\frac{q_1}{q_o} \propto \frac{x}{r_o}\left(\frac{T_o}{T_1}\right)^{\frac{1}{2}} \qquad \ldots.(10)$$

where q_o = primary jet mass flow rate, x = axial length at closure of reversal, q_1 = mass flow rate in jet at x, r_o = radius of primary jet- T_o = temperature of primary jet, T_1 = temperature of entrained gas. If q_1 is large compared with q_o then

$$q = q_R \propto \rho_R V_R R^2 \qquad \ldots.(11)$$

where q_R = reversal mass flow rate, ρ_R = gas density in reversal, V_R = reversal mean velocity and R = radius of reversal core. Then, putting x proportional to R, Equation (10) can now be re-written

$$\rho_R V_R R^2 \propto q_R \propto \frac{q_o R}{r^o}\left(\frac{T_o}{T_1}\right)^{\frac{1}{2}} \qquad \ldots.(12)$$

whence

$$\rho_R V_R \propto \frac{q_o}{r_o R}\left(\frac{T_o}{T_1}\right)^{\frac{1}{2}} \propto \frac{q_o}{A_o}\left(\frac{T_o}{T_1}\right)^{\frac{1}{2}} \quad \ldots.(13)$$

where A_o = area of primary jet.

whence

$$V_R \propto \frac{q_o}{\rho_R A_o}\left(\frac{T_o}{T_1}\right)^{\frac{1}{2}} \quad \ldots.(14)$$

The data of Tables I and II have therefore been recalculated by multiplying the observed reversal mass flow rate by the square root of the temperature ratio (in tests where there was combustion) and by reducing all the data to a standard inlet nozzle area of 100 mm^2. The results are plotted against the inlet (reactants) mass flow rate in Figures 19 and 20.

The results fully confirm the relationship deduced above. The data of Figure 20 for the new design of baseplate indicate that the jet here is operating more efficiently in entraining recirculated gases. A glance at Figure 9 suggests that this may be due to more efficient use of the earlier (high velocity) part of the annular jet.

In addition to tests with the primary air jet alone, tests were also made with the addition of the acoustic atomizer air and the atomizer shroud air, separately and together. The air quantities involved are shown in Table II. It is evident from Figure 20 that this relatively small quantity of low velocity air discharged close to the centre of the baseplate, has little influence on the entrainment process in the primary jet.

5.0 Conclusions

A significant advance in manufacturing technique has permitted the construction of an established design of compact 5-hole spherical velocity vector probe in platinum/rhodium alloy. The resulting probe has been shown to stand up well to prolonged exposure in non-luminous primary zone flames (NB no significant experience with smoky flames has yet been obtained). The further development of the aerodynamic design of this type of probe has led to a new type of 7-hole probe which can accept a vector from any direction in space. During the development work, a series of preliminary velocity vector mapping experiments on model primary zones has been carried out. The results have been shown to accord with what would be predicted by the established theory of jet entrainment.

A commercial design of sensitive micromanometer has been used and tested during this work and has been found to be reasonably robust and of adequately fast response under the conditions of use.

The new probe design lends itself particularly to traversing a cylindrical or annular combustion space by inserting the probe axially from

a point at the centre of the discharge orifice. A traverser of this kind has been designed, incorporating some of the equipment described by D J Fullbrook[14] for semi-automatic three dimensional actuation of aerodynamic probes. This will be used for more detailed mapping of the flow field in these model combustors and the results will be described elsewhere.

ACKNOWLEDGEMENTS

The author would like to pay tribute to the patient skill of the several instrument makers and welders who have built these probes and made the work possible. Thanks are also due to Martin Cox for useful discussions on jet entrainment theory.

REFERENCES

No.	Author(s)	Title, etc.
1	J. J. Macfarlane	Flame Radiation Studies using a model gas turbine primary zone 12th International Symposium on Combustion 1969, pp 1255 to 1264
2	J. J. Macfarlane	To be published
3	A. E. Clarke A. J. Gerrard L. A. Holliday	Some experiences in gas turbine combustion chamber practice using water flow visualization techniques 9th International Symposium on Combustion 1962, pp 878 to 891
4	R. E. W. Janssen	A parametric design study of a laser doppler anemometer to measure turbulence in 150 to 1000 ms^{-1} flows Part I Isotropic turbulence Southampton University Aeronautics and Astronautics Dept Report No. 289, 1970
5	E. Ower	The Measurement of Airflow Chapman and Hall
6	J. C. Lee J. E. Ash	Three-Dimensional spherical pitot probe Trans ASME 1956, Vol 78, pp 603 to 607
7	A. E. S. Pengelley	New Equipment for flame and furnace research J Inst Fuel, 1962, 35, pp 210 to 219
8	J. J. Macfarlane	UK Patent 1207609
9	J. J. Macfarlane	Combustion and Heat Transfer in gas turbine systems Cranfield Symposium No. 11 pp 327 to 339. Edited E. R. Norster Pergamon Press 1971
10	A. E. S. Pengelley	Apparatus for the measurement of gas velocity in furnaces and models J Sci Inst 1960 37 339
11	F. H. Holderness J. R. Tilston J. J. Macfarlane	Electrical Compensation for radiation loss in thermocouples NGTE Note No. NT.758 August 1969
12	M. Cox	Private communication

REFERENCES (cont'd)

No.	Author(s)	Title, etc.
13	F. P. Ricou D. B. Spalding	Measurements of entrainment by axisymmetrical turbulent jets J Fluid Mechanics 1961, 11, 22
14	D. J. Fullbrook	Unpublished work at NGTE

TABLE I

Flat Baseplate Model (Figure 18a)

Annular inlet air nozzle, internal diameter = 60 mm in all cases

Annulus width mm	Annulus area (A) sq mm	q reactants g/s	q reversal g/s	T_o °K	T °K	$\sqrt{\frac{T}{T_o}}$	$\frac{A}{A_o}$ *	q corr g/s
0.20	39.4	7.85	21.89	294	294	1	0.394	8.62
"	"	6.45	18.14	294	294	1	0.394	7.15
"	"	4.97	15.17	294	294	1	0.394	5.98
"	"	3.18	9.12	294	294	1	0.394	3.59
"	"	2.98	3.86	292	1475	2.25	0.394	3.41
"	"	5.42	5.03	292	1850	2.52	0.394	4.98
"	"	1.59	3.89	293	293	1	0.394	1.53
"	"	5.05	4.81	294	1685	2.40	0.394	4.54
"	"	5.02	5.42	294	1530	2.28	0.394	4.87
"	"	0.93	3.10	294	294	1	0.394	1.22
0.48	92.9	5.29	6.36	293	293	1	0.929	5.91
"	"	8.00	9.47	293	293	1	0.929	8.86
"	"	9.20	10.76	293	293	1	0.929	10.00
"	"	2.60	3.28	293	293	1	0.929	3.05
"	"	6.92	8.00	293	293	1	0.929	7.43
"	"	12.00	13.72	293	293	1	0.929	12.75
"	"	13.77	16.39	292	292	1	0.929	15.23
"	"	15.18	17.63	290	290	1	0.929	16.38
"	"	9.71	4.12	295	1871	2.52	0.929	9.66
"	"	5.86	2.19	294	1659	2.44	0.929	4.95
"	"	5.90	2.41	292	1839	2.51	0.929	5.62
"	"	5.99	2.22	291	1562	2.32	0.929	4.77
"	"	6.18	2.04	291	2102	2.69	0.929	5.08
"	"	10.30	3.88	291	2212	2.76	0.929	9.95
"	"	14.95	7.19	293	1740	2.44	0.929	16.30
0.69	132.3	10.20	8.11	298	298	1	1.323	10.72
"	"	15.77	12.06	298	298	1	1.323	15.95
"	"	21.30	15.80	299	299	1	1.323	20.9
"	"	10.99	2.30	297	1830	2.47	1.323	7.5
"	"	14.91	3.46	298	1755	2.44	1.323	11.1

*A_o = 100 sq mm

TABLE II

High Velocity Model

Annulus area A = 89.2 sq mm

All tests in cold flow only

q annulus g/s	q atomizer g/s	q shroud g/s	q reversal g/s	q corr g/s
12.00	-	-	31.63	28.21
5.69	-	-	15.74	14.04
11.97	2.30	-	29.40	26.22
5.89	2.33	-	18.89	16.85
7.20	-	-	19.56	17.45
7.28	2.65	-	19.94	17.79
7.34	-	1.82	18.26	16.29
5.21	-	1.85	13.25	11.82
11.97	-	1.85	29.41	26.23
11.98	2.38	1.85	29.44	26.26

A_o = 100 sq mm

List of symbols

Given in the order in which they first appear in the text.

K	pressure recovery factor (non-dimensional) (also known as the static pressure coefficient)
θ	the angle between the axis of a pressure tapping and the flow direction
δ	the dihedral angle between the radial plane containing the flow direction and a meridian plane of the spherical head of the probe
p	pressure (kg/m^2)
V	velocity (m/s)
ρ	gas density (kg/m^3)
g	the gravitational constant ($9.806\ m/s^2$)
q	gas mass flow rate (kg/s)
x	axial distance from jet (m)
r	radius of primary jet (m)
T	temperature (K)
R	radius of core of flow reversal (m)
A	area of primary jet (m^2)

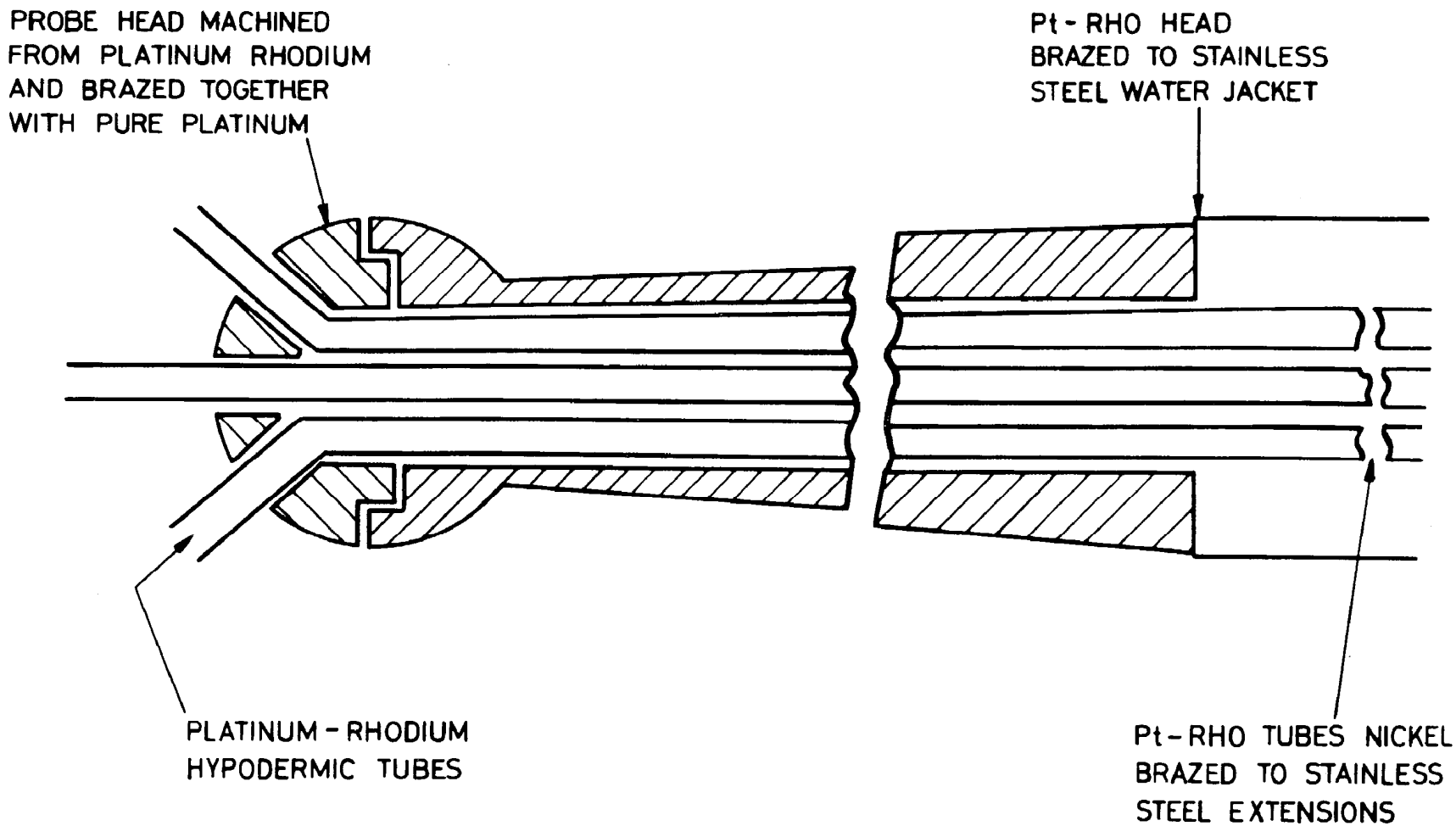

FIG. 1 METHOD OF PROBE CONSTRUCTION

FIG. 1

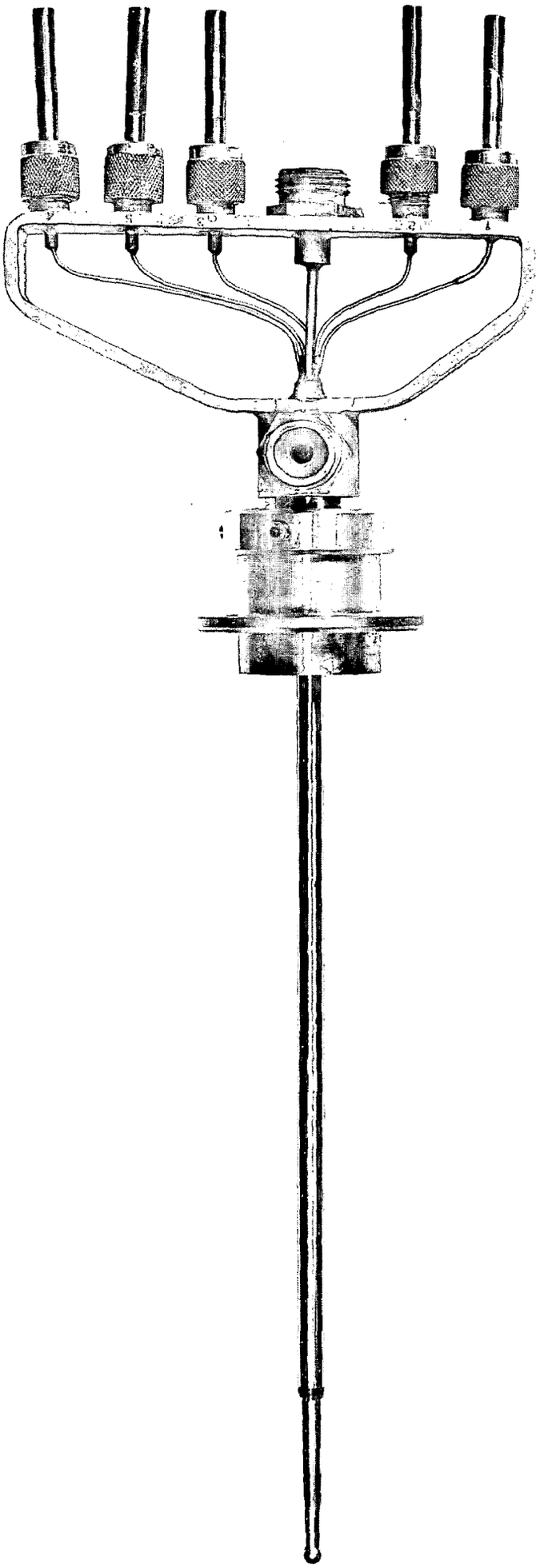

FIG.2 5-POINT PROBE ASSEMBLY

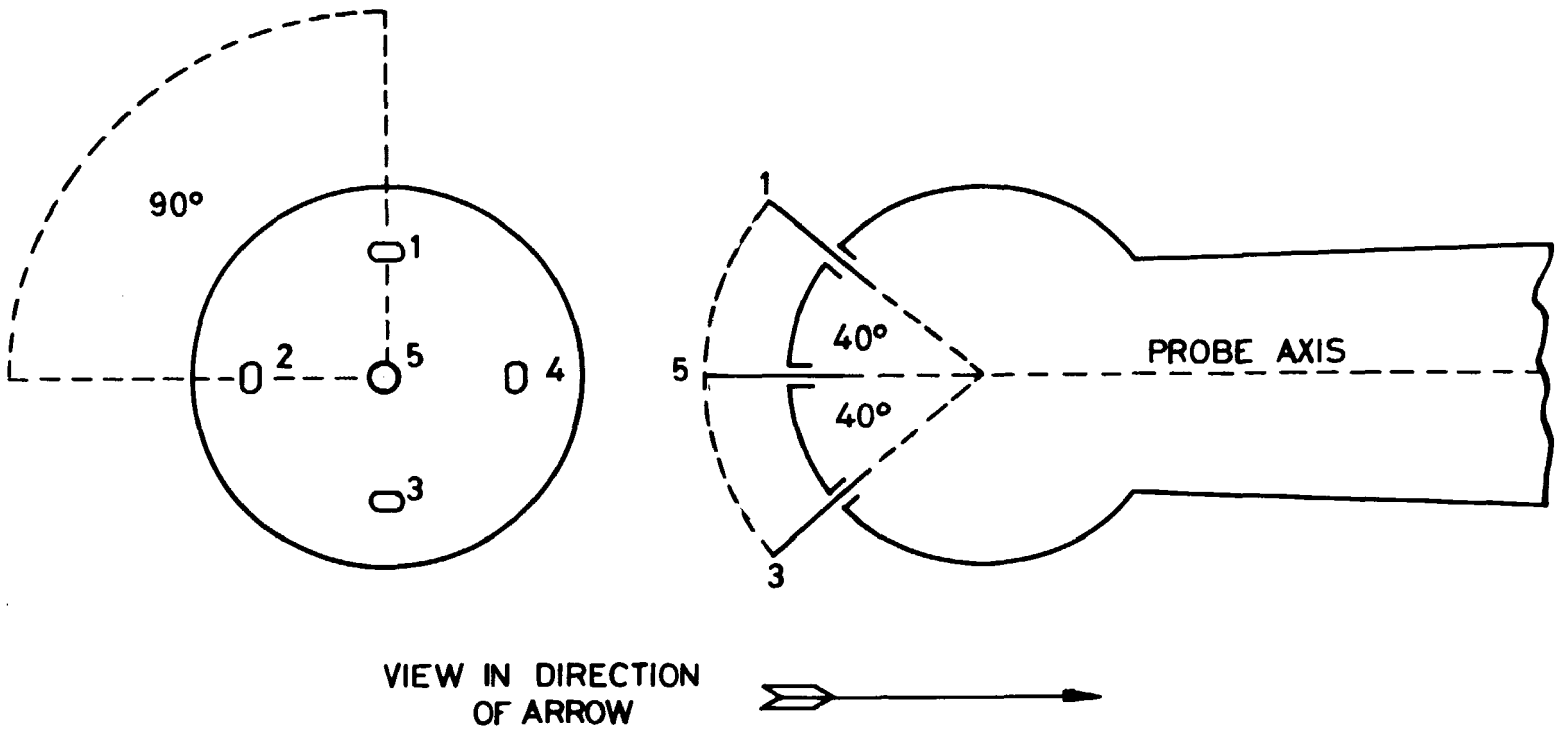

FIG. 3 ARRANGEMENT OF PRESSURE POINTS ON LEE & ASH PROBE

FIG. 3

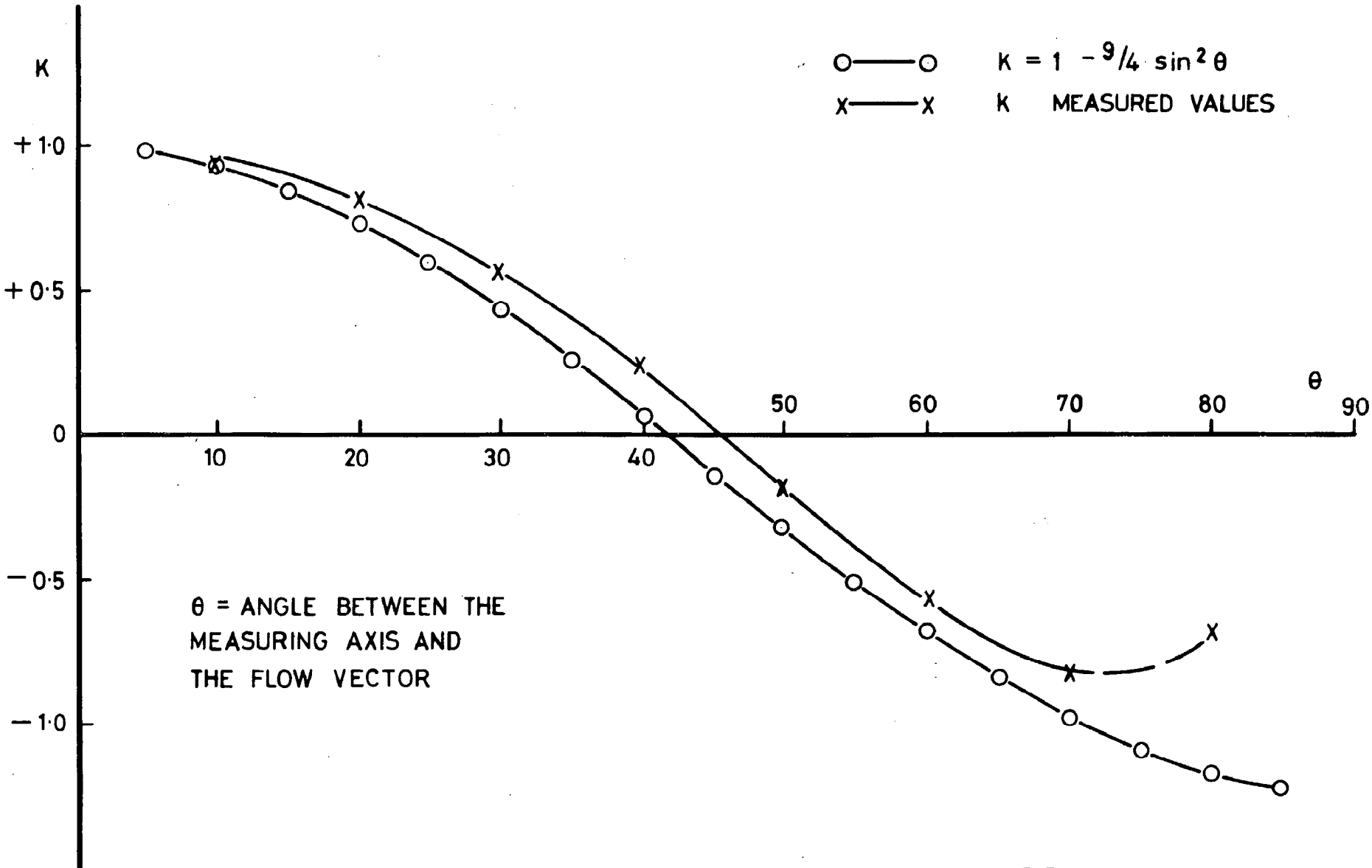

FIG.4 PRESSURE RECOVERY FACTOR AT A POINT ON A SPHERE

FIG.4

SK 107061

FIG. 5

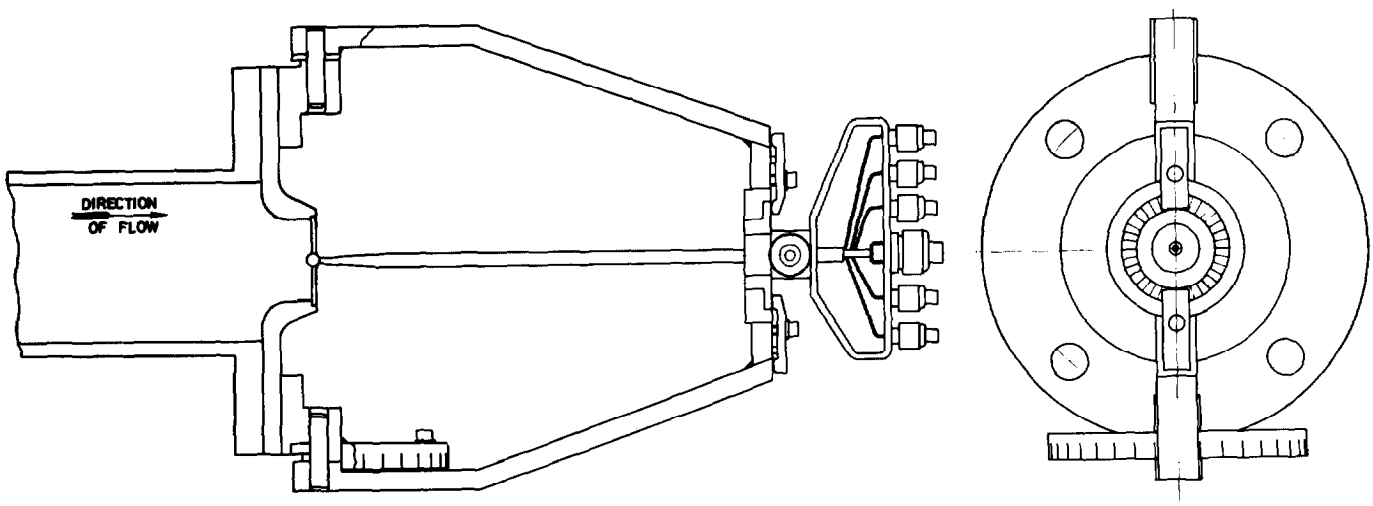

FIG. 5 NOZZLE TYPE CALIBRATION RIG

FIG. 6

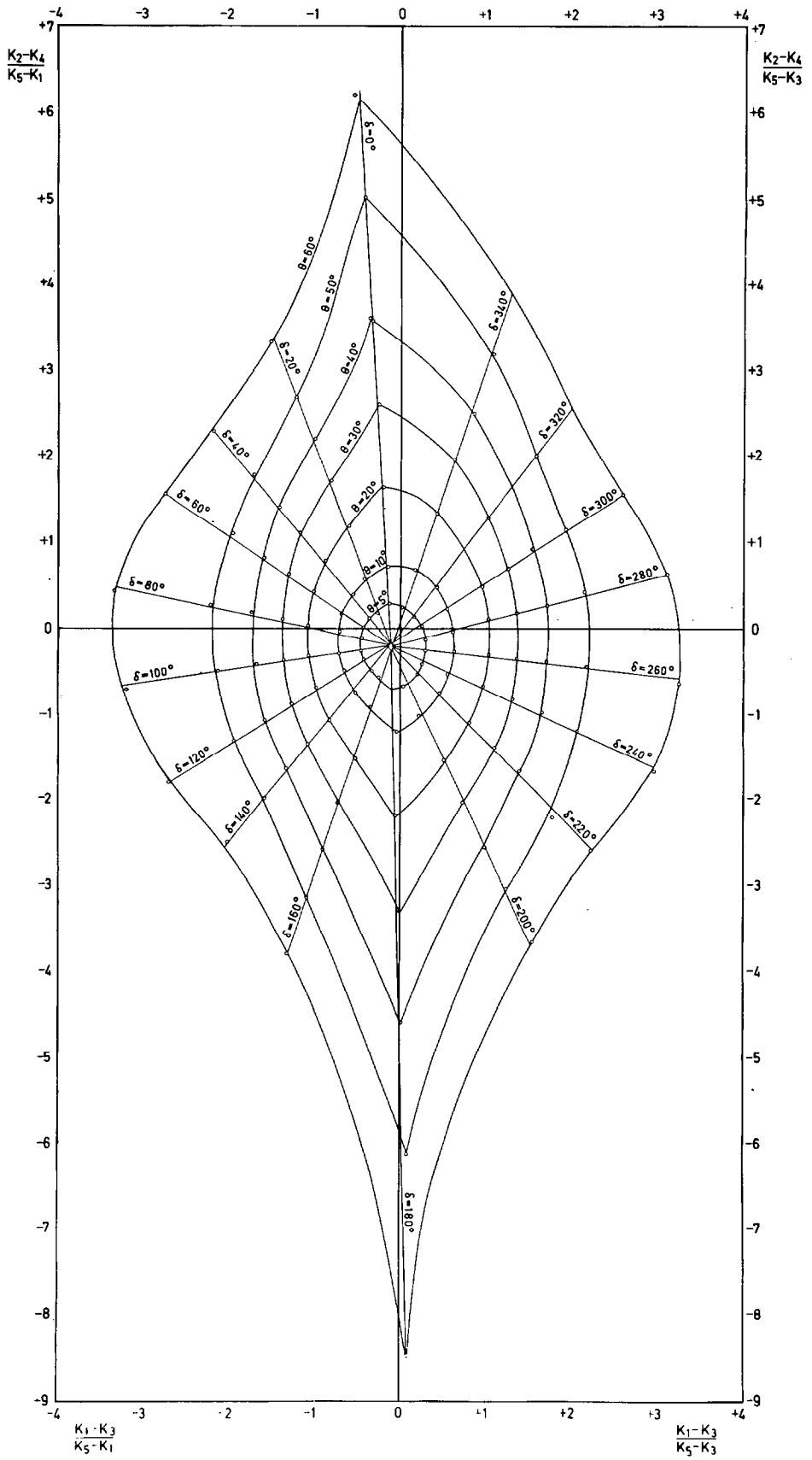

FIG. 6 LEE AND ASH PROBE CALIBRATION

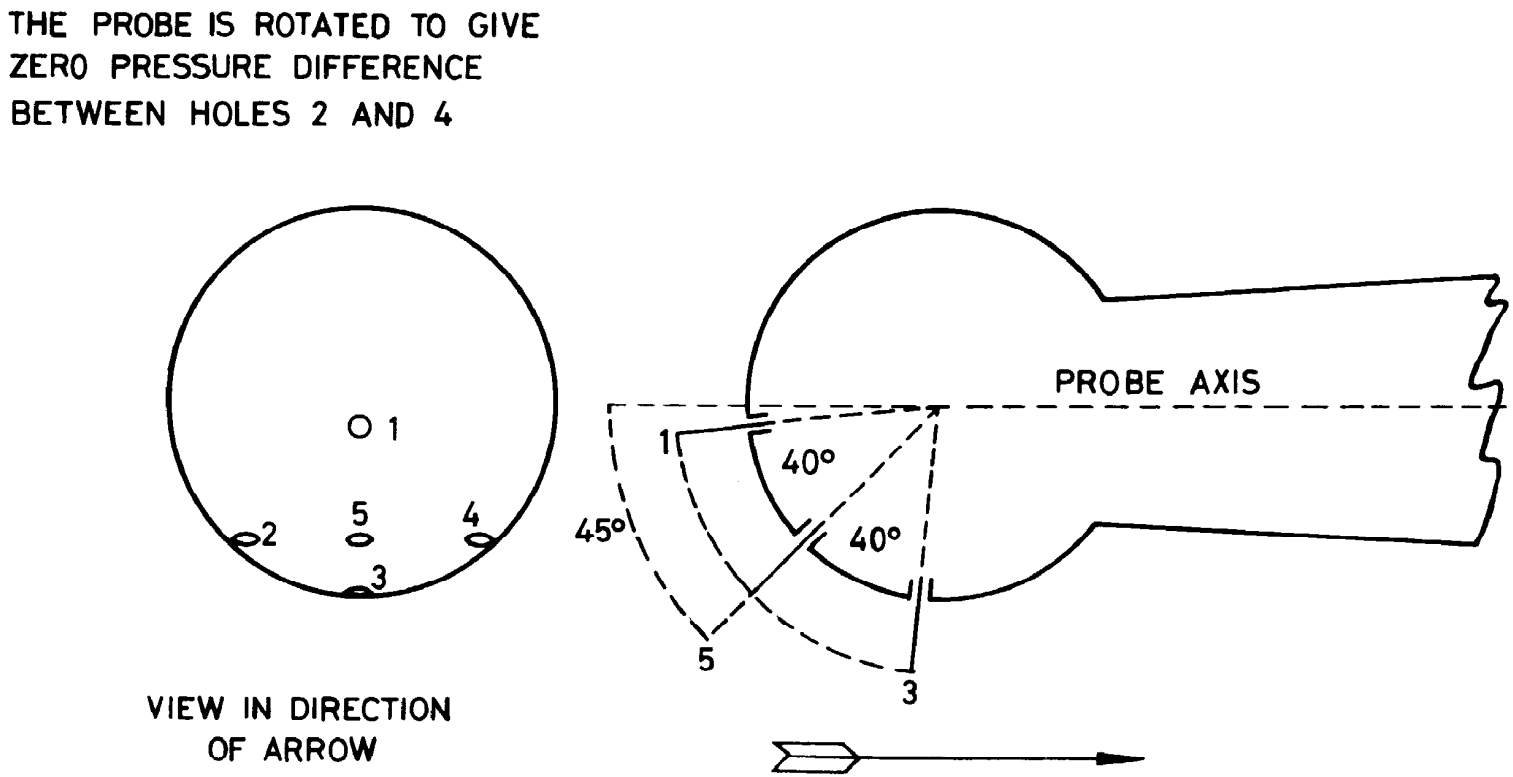

FIG. 7 ARRANGEMENT OF PRESSURE POINTS ON MODIFIED 45° PROBE

FIG.7

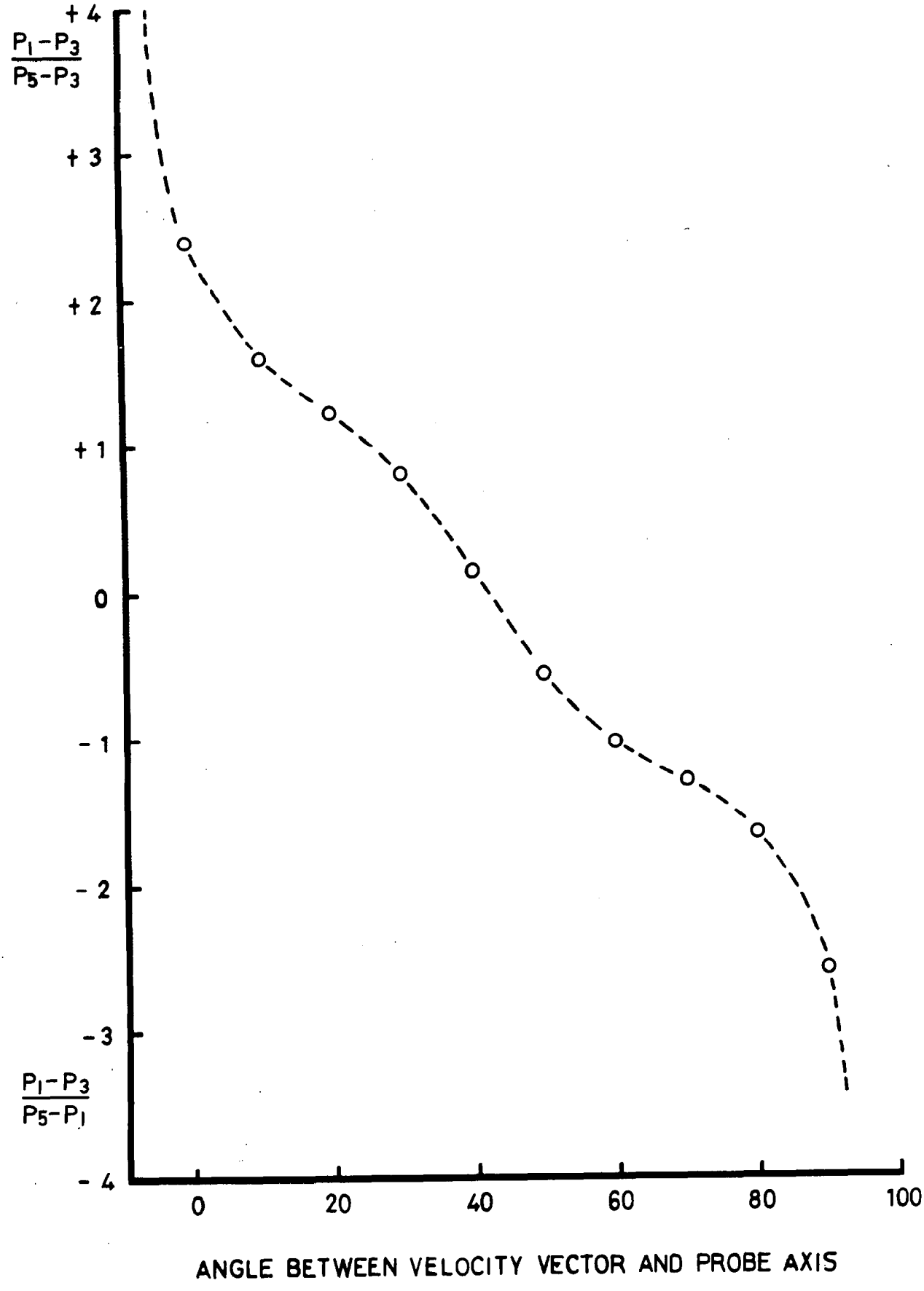

FIG.8 CALIBRATION CURVE FOR 45° PROBES

SK 107062

FIG. 9

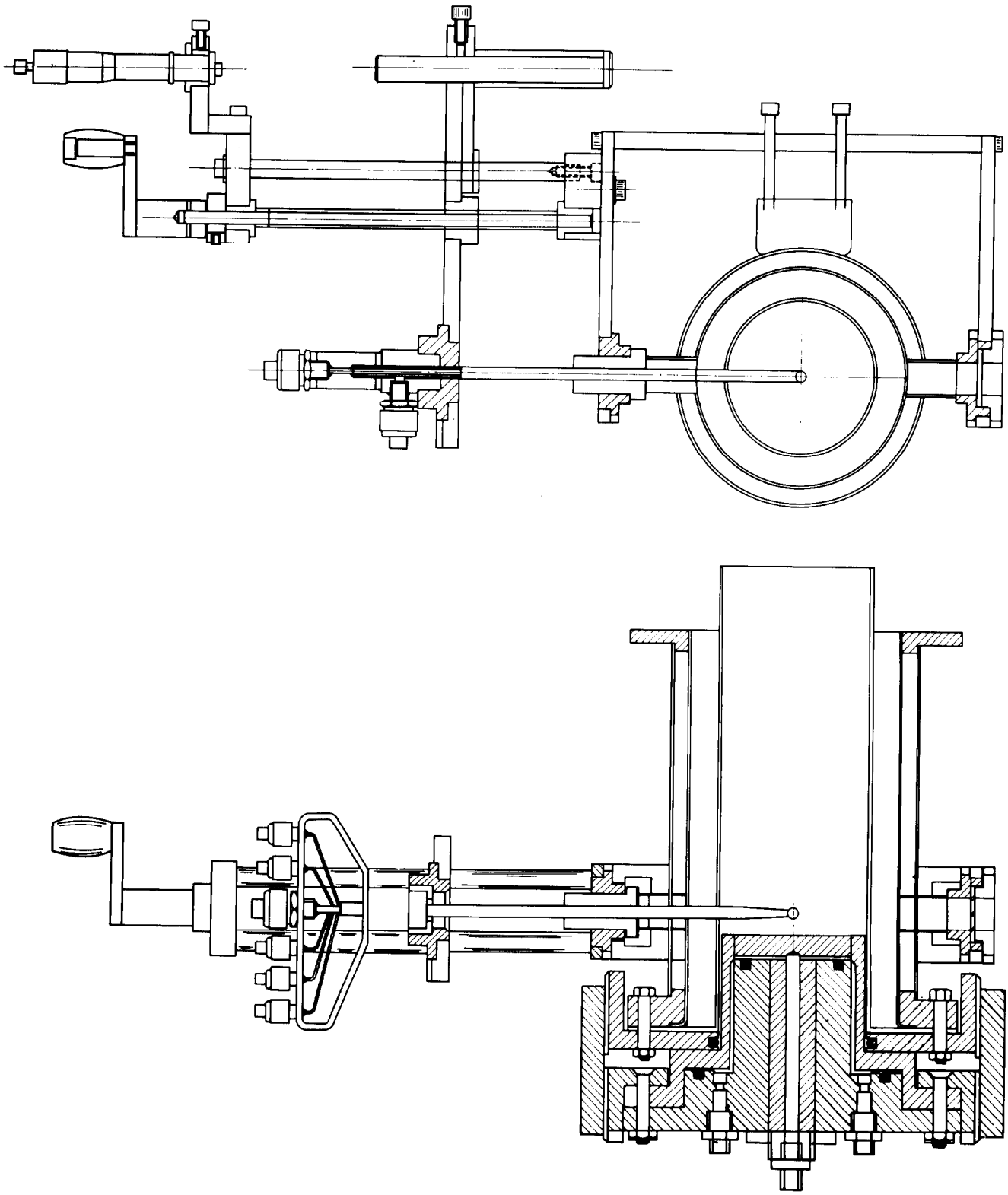

FIG. 9 FIVE POINT PROBE RADIAL TRAVERSER IN PRIMARY ZONE MODELS

FIG. 10

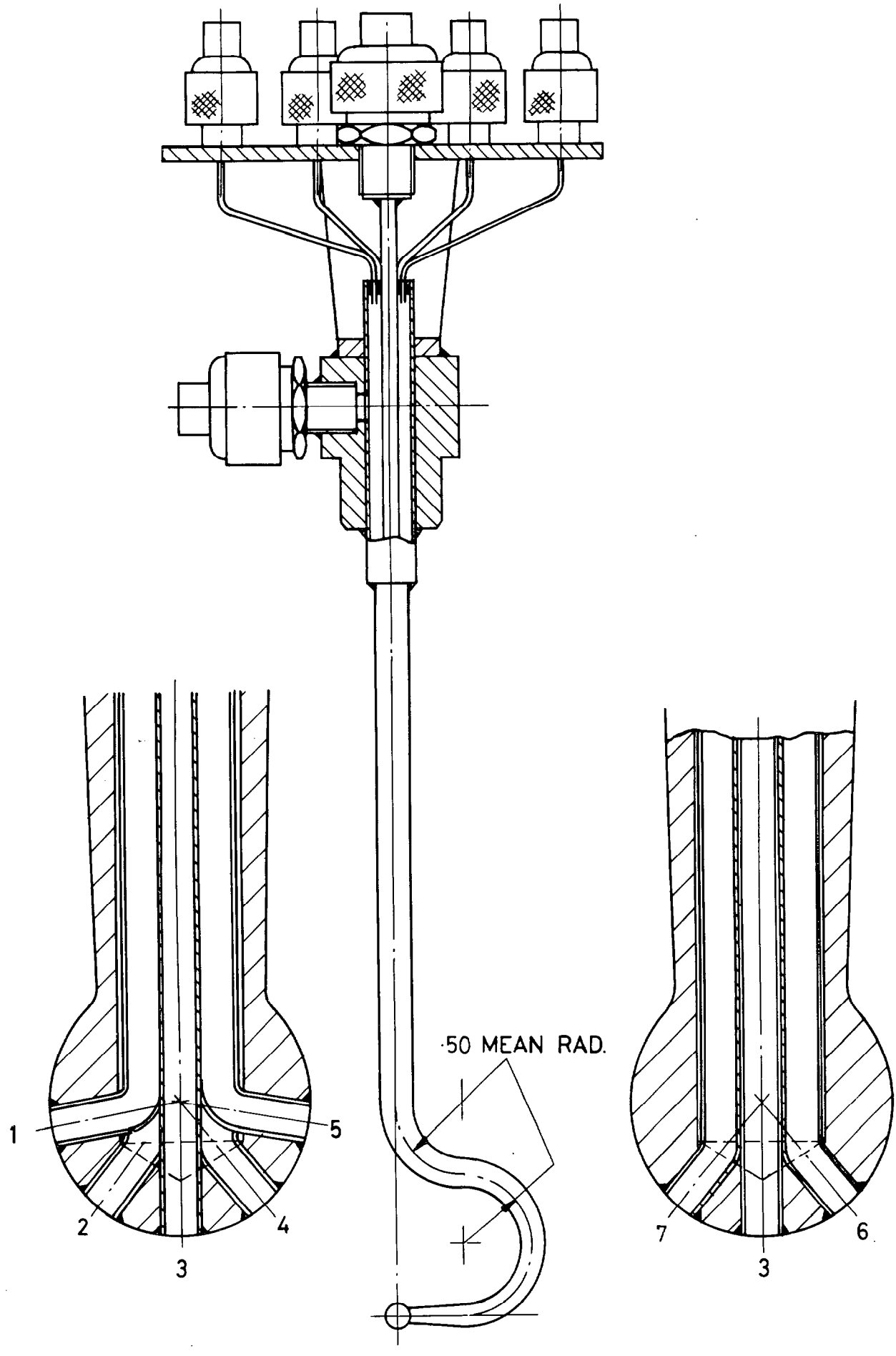

FIG. 10 THE 7 POINT SHEPHERD'S CROOK PROBE

FIG.11

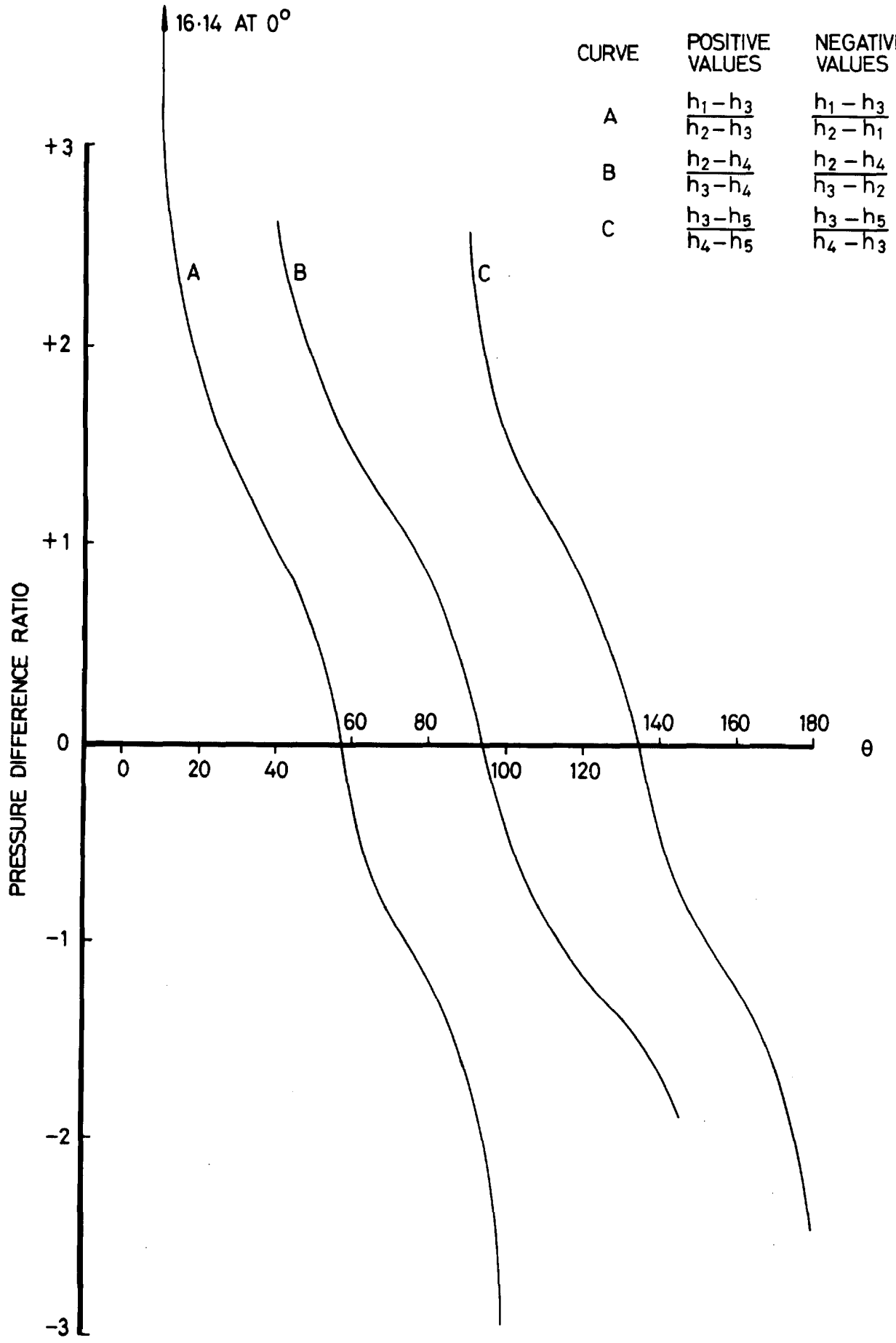

FIG.11 CALIBRATION CURVE FOR 7-POINT SHEPHERDS CROOK PROBE

FIG. 12

SK 107065

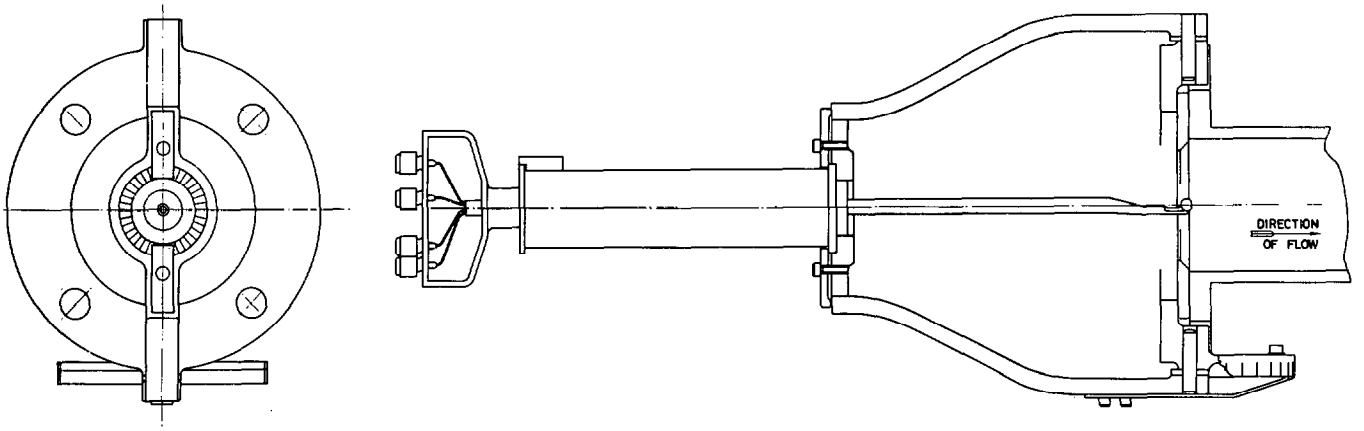

FIG. 12 CALIBRATION JIG FOR SEVEN POINT PROBE USING A SUCTION SOURCE

FIG.13

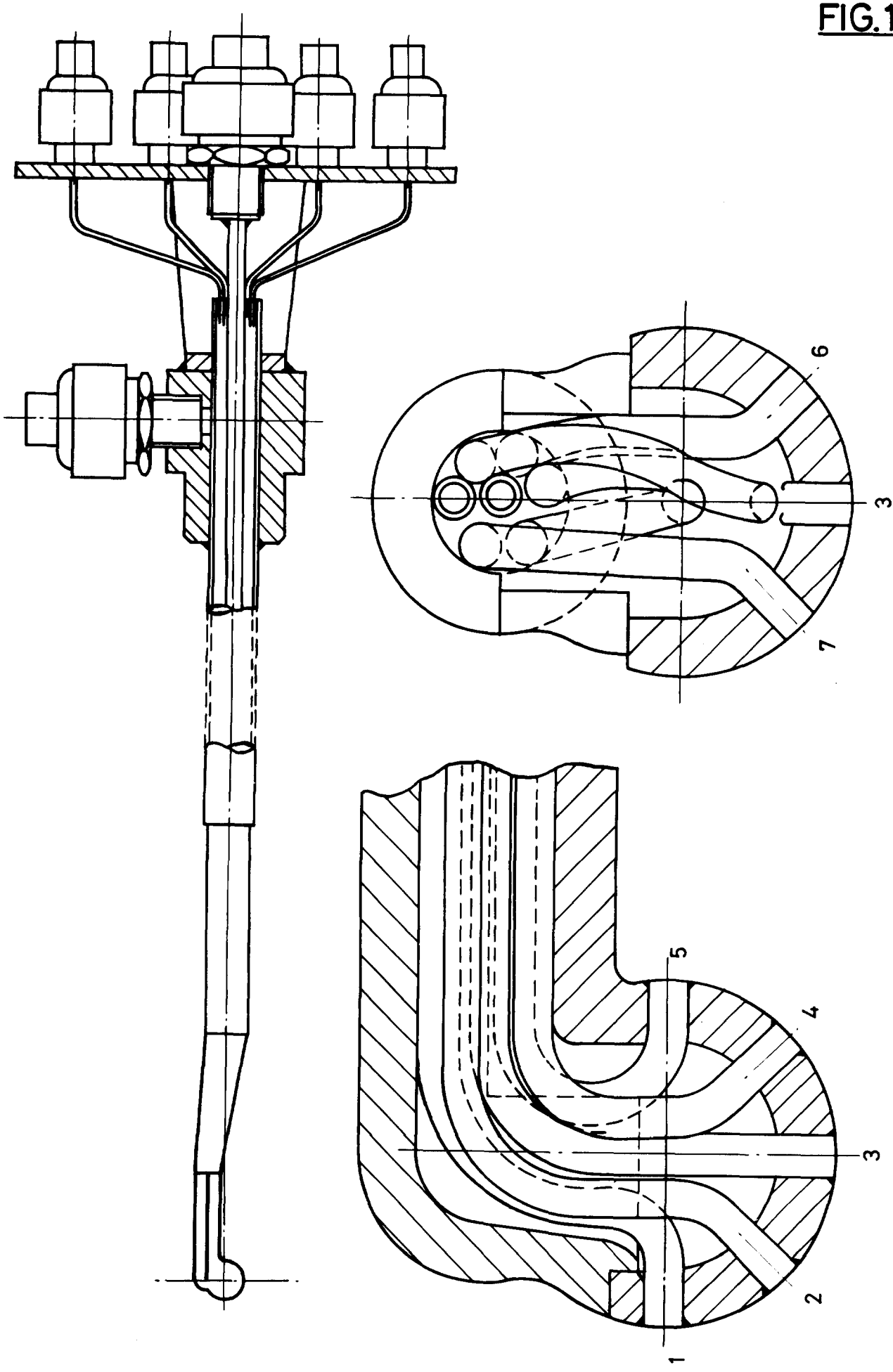

FIG. 13 7 POINT SPHERICAL PROBE
(PREFERRED FORM WITHOUT CROOK)

SK 107067

FIG. 14

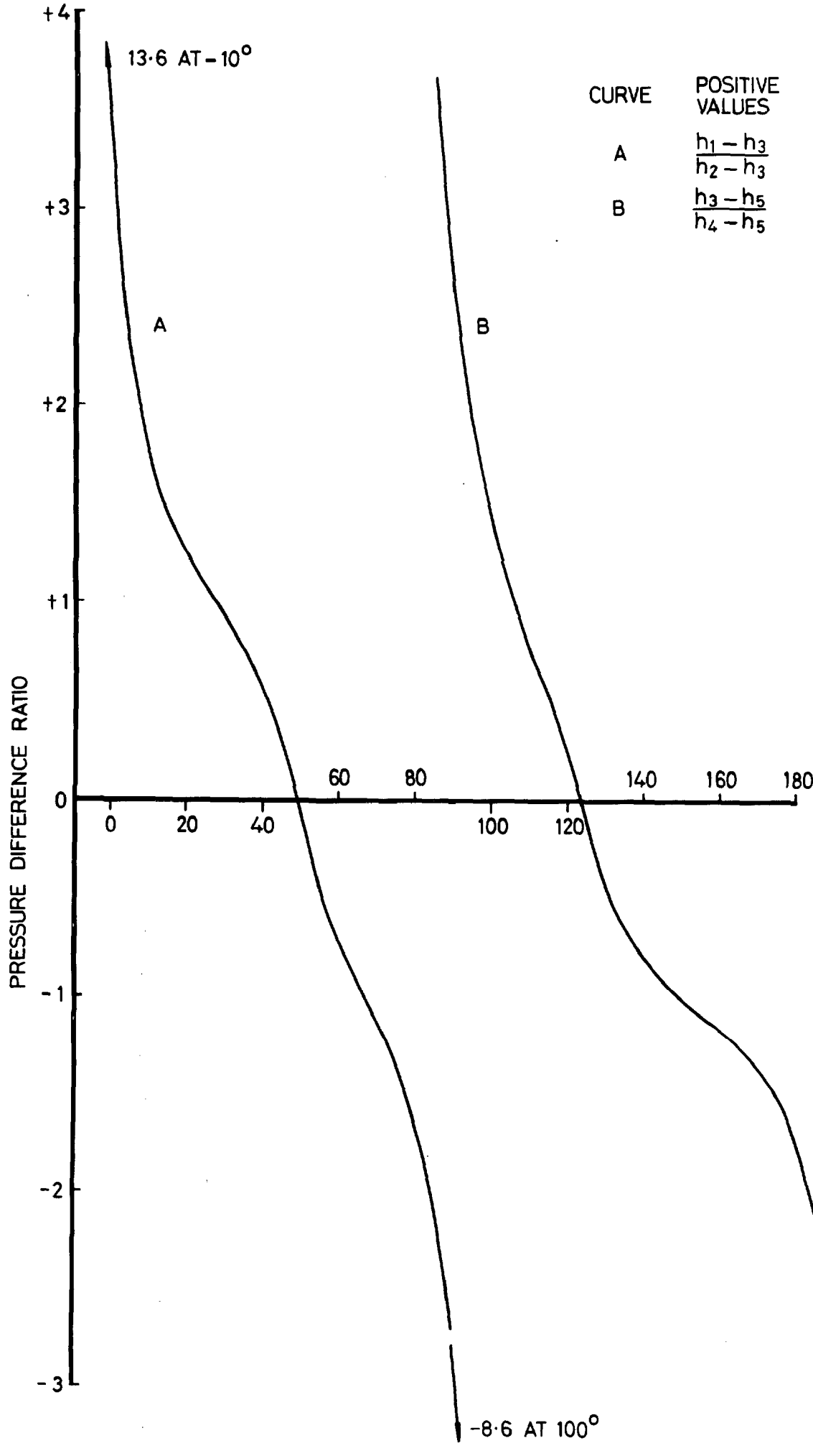

FIG.14 CALIBRATION CURVE FOR 7-POINT PROBE WITHOUT CROOK

FIG. 15

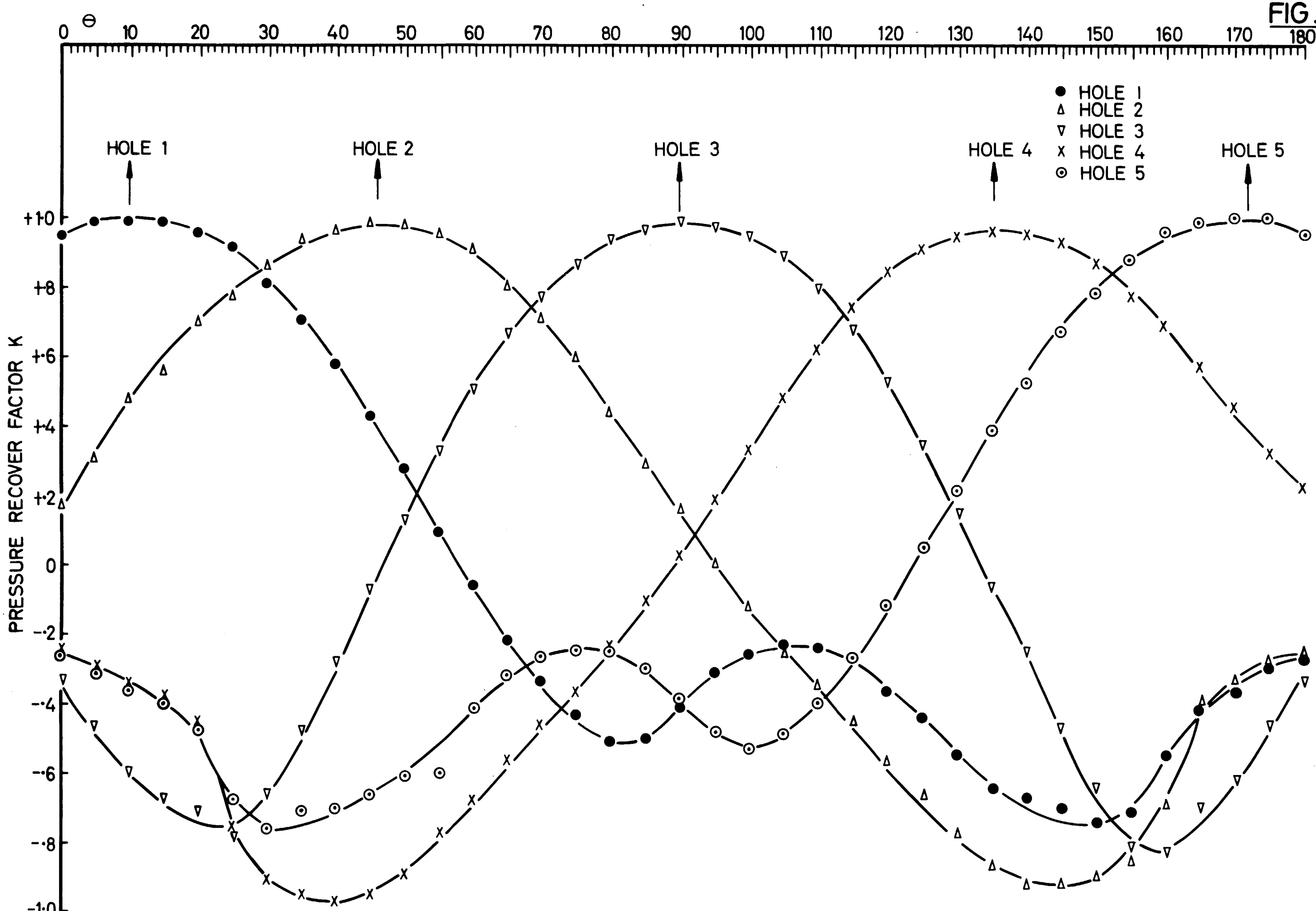

FIG. 15 PRESSURE RECOVERY FACTORS FOR HOLES 1 TO 5 OF A 7 POINT PROBE, SHOWING MIS-LOCATION OF HOLES 1 AND 5

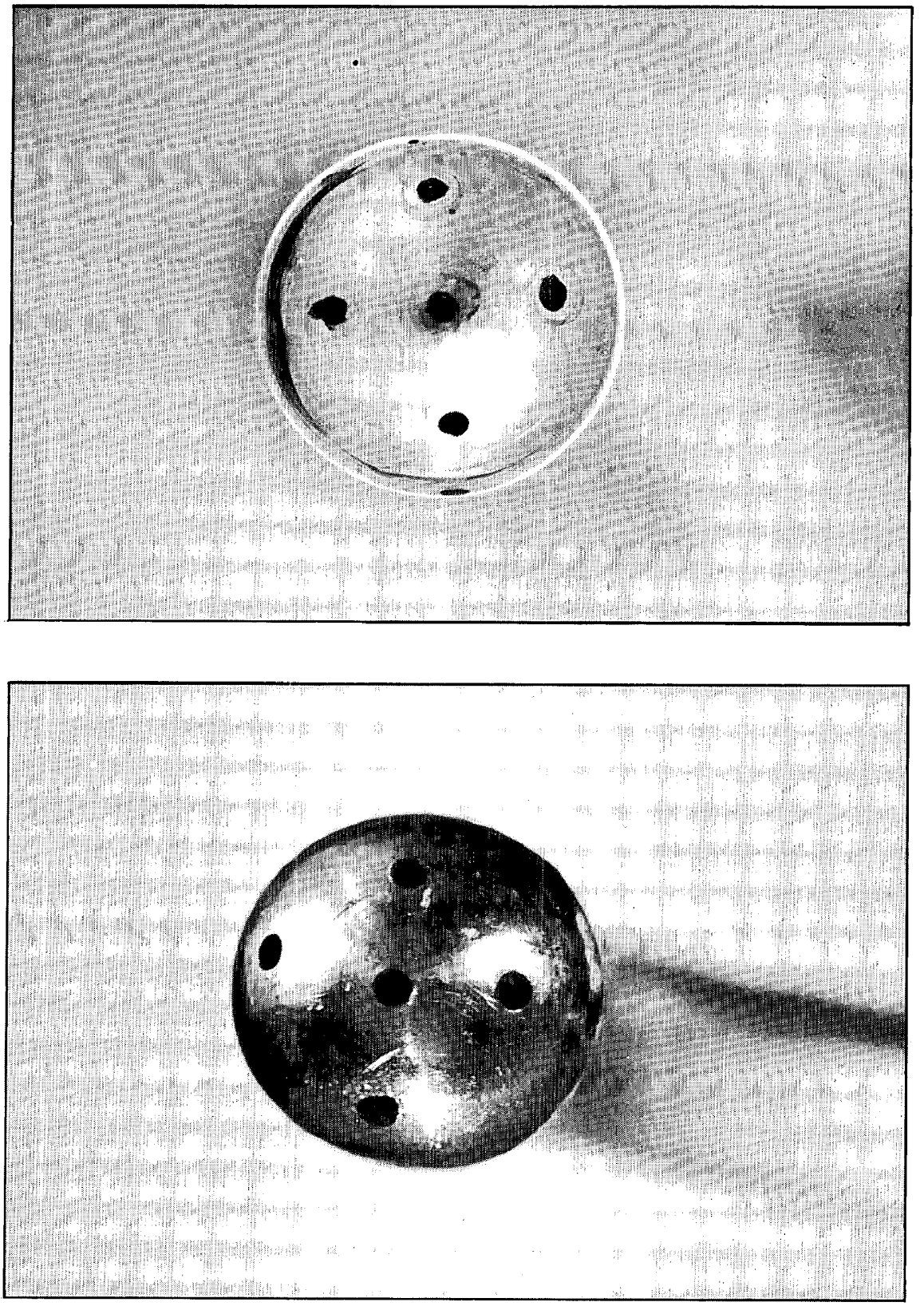

FIG. 16 COMPARISON OF WELL MADE AND FAULTY PROBE HEADS

SK. 107069

FIG.17

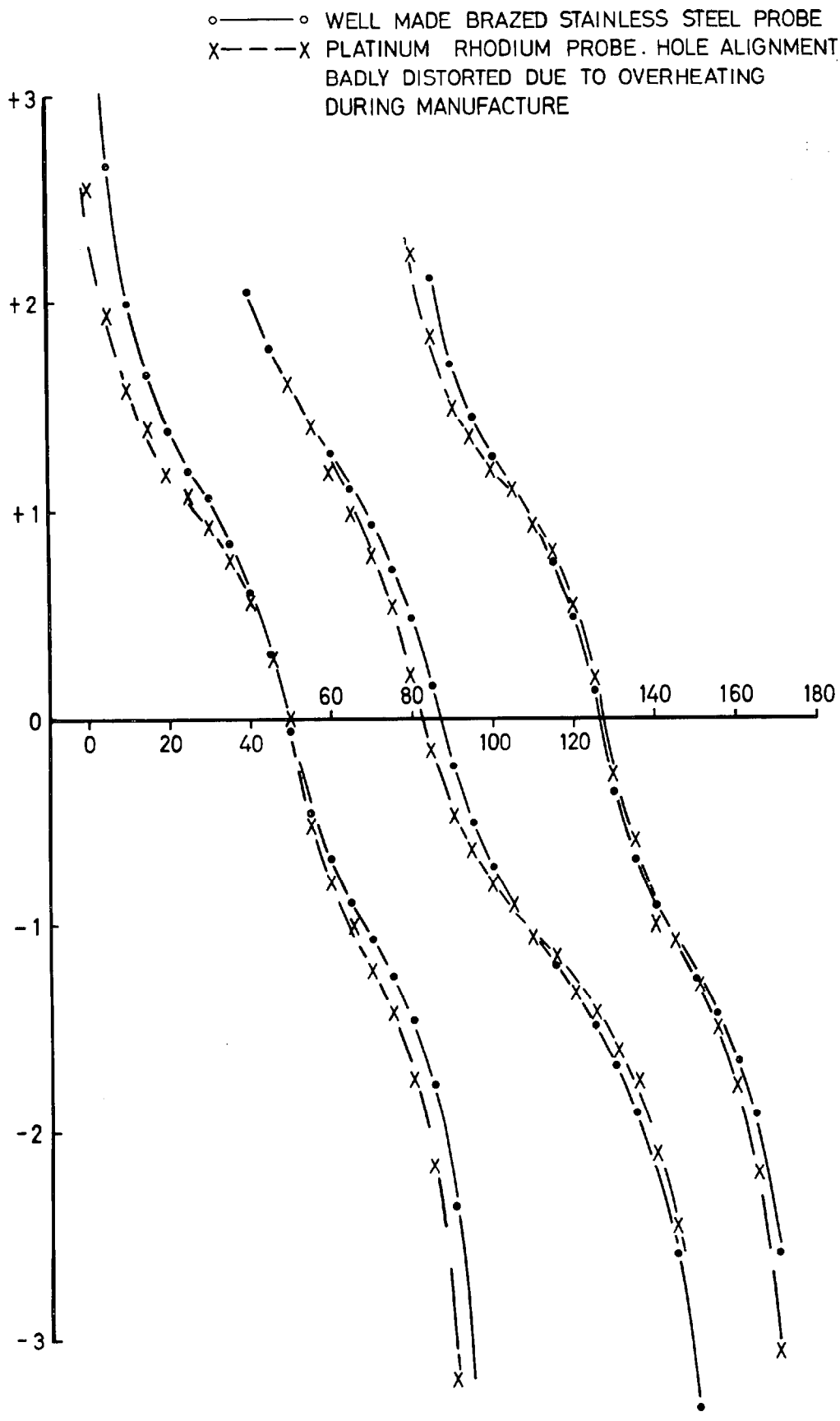

FIG.17 COMPARISON OF CALIBRATION CURVES FOR THE TWO PROBES SHOWN IN FIGURE 16

FIG. 18

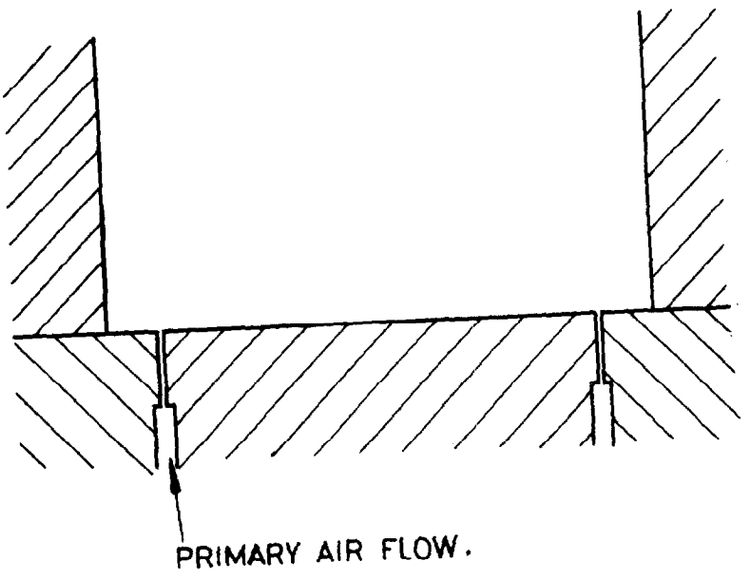

(a) FLAT BASEPLATE MODEL

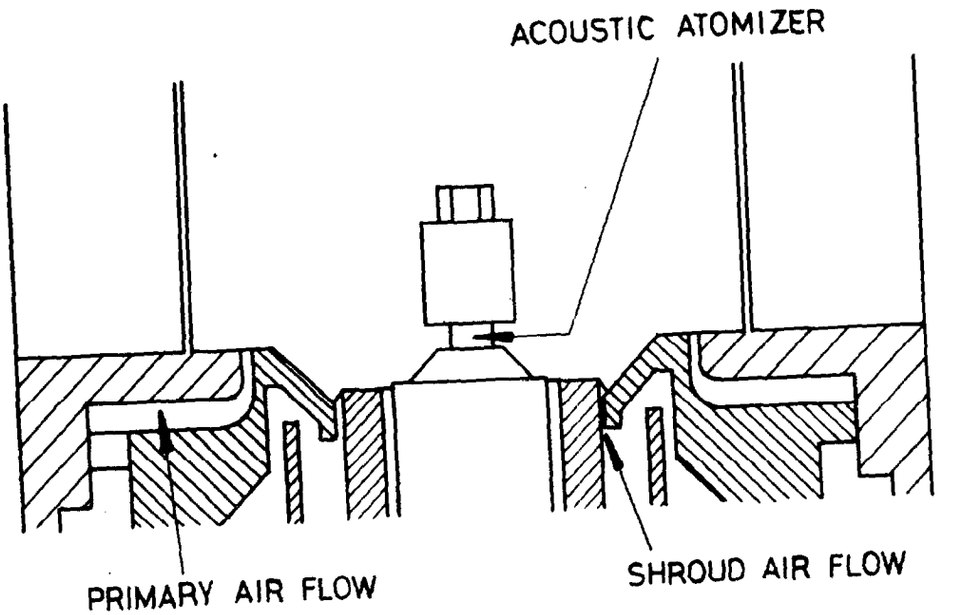

(b) HIGH VELOCITY MODEL

FIG. 18 DETAILS OF ARRANGEMENTS OF BASEPLATES OF MODEL COMBUSTORS USED FOR VELOCITY VECTOR TRAVERSING

ARC CP No.1254
October, 1971
Macfarlane, J. J.

AN OMNI-DIRECTION VELOCITY VECTOR PROBE SUITABLE FOR USE IN GAS TURBINE COMBUSTORS; DESIGN DEVELOPMENT AND PRELIMINARY TESTS IN A MODEL COMBUSTOR

A new technique is described which permits the construction of spherical multi-hole velocity vector probes in platinum/20% rhodium alloy. These probes are shown to be suitable for use at gas turbine primary flame temperatures while the head is sufficiently compact to permit the probe to be used in model combustor research. Starting with an established design of 5-hole probe, a programme of development is described which has led to a new/

ARC CP No.1254
October, 1971
Macfarlane, J. J.

AN OMNI-DIRECTION VELOCITY VECTOR PROBE SUITABLE FOR USE IN GAS TURBINE COMBUSTORS; DESIGN DEVELOPMENT AND PRELIMINARY TESTS IN A MODEL COMBUSTOR

A new technique is described which permits the construction of spherical multi-hole velocity vector probes in platinum/20% rhodium alloy. These probes are shown to be suitable for use at gas turbine primary flame temperatures while the head is sufficiently compact to permit the probe to be used in model combustor research. Starting with an established design of 5-hole probe, a programme of development is described which has led to a new/

ARC CP No.1254
October, 1971
Macfarlane, J. J.

AN OMNI-DIRECTION VELOCITY VECTOR PROBE SUITABLE FOR USE IN GAS TURBINE COMBUSTORS; DESIGN DEVELOPMENT AND PRELIMINARY TESTS IN A MODEL COMBUSTOR

A new technique is described which permits the construction of spherical multi-hole velocity vector probes in platinum/20% rhodium alloy. These probes are shown to be suitable for use at gas turbine primary flame temperatures while the head is sufficiently compact to permit the probe to be used in model combustor research. Starting with an established design of 5-hole probe, a programme of development is described which has led to a new/

ARC CP No.1254
October, 1971
Macfarlane, J. J.

AN OMNI-DIRECTION VELOCITY VECTOR PROBE SUITABLE FOR USE IN GAS TURBINE COMBUSTORS; DESIGN DEVELOPMENT AND PRELIMINARY TESTS IN A MODEL COMBUSTOR

A new technique is described which permits the construction of spherical multi-hole velocity vector probes in platinum/20% rhodium alloy. These probes are shown to be suitable for use at gas turbine primary flame temperatures while the head is sufficiently compact to permit the probe to be used in model combustor research. Starting with an established design of 5-hole probe, a programme of development is described which has led to a new/

DETACHABLE ABSTRACT CARDS

new design of 7-hole probe which can accept a vector from any direction in space. Tests were made in model primary zones to validate certain features of this design during its development and the results of these are described and discussed.	new design of 7-hole probe which can accept a vector from any direction in space. Tests were made in model primary zones to validate certain features of this design during its development and the results of these are described and discussed.
new design of 7-hole probe which can accept a vector from any direction in space. Tests were made in model primary zones to validate certain features of this design during its development and the results of these are described and discussed.	new design of 7-hole probe which can accept a vector from any direction in space. Tests were made in model primary zones to validate certain features of this design during its development and the results of these are described and discussed.

HER MAJESTY'S STATIONERY OFFICE

Government Bookshops

49 High Holborn, London WC1V 6HB
13a Castle Street, Edinburgh EH2 3AR
109 St Mary Street, Cardiff CF1 1JW
Brazennose Street, Manchester M60 8AS
50 Fairfax Street, Bristol BS1 3DE
258 Broad Street, Birmingham B1 2HE
80 Chichester Street, Belfast BT1 4JY

Government publications are also available through booksellers

C.P. No. 1254

SBN 11 470812 6